An Improved Bulk Viscosity Method for Contact-Impact Problems

Balázs Pere, Dániel Serfőző

Széchenyi István University, Egyetem tér 1, 9026 Győr, Hungary
pere.balazs@ga.sze.hu; serfozo.daniel@sze.hu

Abstract: Dynamic contact and impact problems are widely applicable. An accurate solution for these kinds of problems could be used in many fields of mechanical engineering (e.g., cutting metalwork, cogwheel drives, etc.). However, the proper handling of the contact is problematic, as there emerges a substantial amount of nonlinearity in the displacement field. Therefore, a spurious high frequency oscillation is present in the solution. These oscillations must be avoided, as divergence can easily occur in the contact algorithm due to them. In order to eliminate this effect, the applied numerical method must be chosen and set properly. In this study, we focused on the best possible elimination of these oscillations by which the choice of the proper numerical method has a great importance.

Keywords: numerical method; contact; impact; oscillation; wave propagation

1 Introduction

Engineering structures often contain parts which are in contact. Even today, solving contact problems is one of the most challenging tasks in numerical analysis of structures. On one hand, the difficulty of such problems results from its non-linear nature. On the other hand, inaccuracy raising from the discretization of a continuum as a set of distinct points can also cause problems. The first contact problem was solved by Hertz in 1881 [1]. He determined the contact area and the distribution of the contact pressure of two elastic spheres analytically. There are very few problems involving contact which can be solved in an analytical way. With the growing power of modern computers, the Finite Element Method (FEM) evolved and has become capable to give approximate solutions for problems arising from elasticity. FEM was firstly used for solving contact problems in the mid 70's (see [2]). The application of finite element (FE) analysis for contact problems has a vast literature [3]. The simplest, fastest, but less accurate method for solving mechanical contact problems with FE codes is the *penalty method* where a relatively big penalty parameter ensures that penetration between the contacting bodies remains small compared to their sizes [4]. The *Lagrange multiplier method* [5] uses the contact pressure as an additional unknown field. It accurately satisfies the contact boundary

conditions, i.e., there is no penetration at the contact interface, but the computation requires more resources, even in the static case. Combination of the aforementioned methods results the *augmented Lagrangian method* [6] which is a good compromise between the penalty and the Lagrange multiplier methods. The main drawback of the augmented Lagrangian method is the applied double loop iteration in the algorithm. All of the aforementioned methods can be utilized for dynamic simulations of structures.

Solution of a dynamic problem usually means time integration of the semi-discretized equation of motion. This semi-discretized equation is discretized in space, but continuous in time. Discretization and integration in time of such an equation can be performed with either implicit or explicit methods [7]. In implicit methods time step can be much bigger than the period of the highest eigenfrequency, while the solution remains numerically stable. The most commonly used implicit method in FE software is the Newmark method [8]. The formula of this method contains a parameter whose change directly affects the numerical damping of the method. An extension of Newmark method is the HHT-α method [9]. This method strongly dissipates the high frequency oscillations while it has moderate dissipation in lower frequencies. The level of dissipation can be controlled with two parameters. By the proper choice of parameters, the implicit method can be switched into explicit, where the dissipation can be also controlled [10]. Noh et al. [11] compared the Bathe method with other existing methods. The properties of the method are very favorable, but oscillations occur, even if only to a small extent. These methods are not suitable to follow sudden changes (like collision of bodies) and to solve vibrations whose frequency is close to the highest eigenfrequency. In contrast, explicit methods, such as central difference method (CDM), can solve contact-impact problems within a reasonable time and accuracy. Here, time step size has to be usually smaller than the period of the highest eigenfrequency, but unlike the implicit method, computation of one-time step can be much faster. CDM is effective when a lumped mass matrix is applied instead of a consistent mass matrix. Krieg and Key showed that lumped mass matrix with explicit methods is ideal because the discretization errors are compensated [12].

Various time-stepping methods keep being developed nowadays. Numerous publications provide techniques to increase the accuracy of solutions for contact-impact problems. The main problem is that in case of collision of bodies, the solution strongly oscillates. This oscillation has no physical background, but it comes from the discretization itself.

One branch of the development is trying to improve the accuracy of time stepping methods. To solve hydrodynamic shock wave propagation problems, a viscous pressure term has been added to the dynamic equations. This approach has been described by Benson [13] and also known as VonNeumann's artificial viscosity method [14]. The bulk viscosity method is based on the explicit central difference method which itself has no numerical dissipation. Here, one parameter – the viscosity – can be used to control the dissipation and reduce oscillations at the same

time. This method is widely used in industrial codes like Abaqus [15] or [16] LS-Dyna. Another method with similar result is the Tchamwa-Wielgosz scheme [17], where also one parameter is needed for the dissipation control. The latter method, in contrast to the bulk viscosity method, is sensitive to the mesh irregularities [18]. Shing and Mahin introduced a modified Newmark-method which, based on their results, proves to be more reliable than the initial stiffness dependent viscous damping when a system is non-linearly elastic [19]. Kolay and Ricles developed an explicit (KR-α) method [20] which is unconditionally stable. The amount of numerical damping is controllable by a single parameter. The numerical damping in the lower mode response is negligible, as well as in the previously mentioned method by Shing and Mahin. Chang [21] has shown that the KR-α method is unable to realistically reflect the dynamic loading. Kim uses a two-stage method with dissipation control capability [22]. Even though his method is more accurate than the others, spurious oscillations are still present, but only to a lesser extent. Kim also applied some parameters to control the numerical dissipation of his method.

In another branch, the contact method is modified in order to dampen the oscillations. Chen et al. applied displacement, velocity and acceleration constraints under persistent contact [23]. It seems from the results that the oscillations have not been reduced significantly. Zhu and Li developed a parametric quadratic programming method which does not require artificial damping to reduce high frequency oscillations [24]. Otto et al. tried to smoothen out the sudden change in contact force utilizing a regularized penalty parameter [25]. This means the smooth increase of the contact pressure during the impact.

In this article, a different, novel approach is presented to reduce the spurious oscillations. Many papers so far have used increasingly clever methods to find a more precise solution. Newer and newer parameters are introduced into the equations to try to control the numerical damping in ever more sophisticated ways. The methods are sorted by some indicators, like numerical dispersion, dissipation, period elongation and amplitude decay. In contrast to the existing methods, our idea was to determine the optimal damping characteristic of a time stepping method at first. The best existing methods are not efficient enough, dissipate too much energy at low frequencies and too little at high frequencies.

The rest of the paper is organized as follows. Section 2 presents some widely used time stepping numerical methods, while Section 3 gives an accuracy analysis of them. In Section 4, a one-dimensional FE model is introduced, which can demonstrate the efficiency of the proposed method discussed in Section 5. Section 6 shows a numerical example to compare the previously presented and the proposed methods. In Section 7 some conclusions are drawn concerning the overall results.

2   Time Stepping Methods with Damping Effects

The initial step in solving dynamic contact problems is to formulate the semi-discretized equation of motion. In this paper, it is assumed that the strains are small and the material behaves linearly elastic. The discretization in space can be performed using e.g., FEM which leads to the following matrix equation.

$$\mathbf{M\ddot{u} + Ku = f} \tag{1}$$

where $\mathbf{M}$ is the mass matrix, $\mathbf{K}$ is the stiffness matrix, $\mathbf{f}$ is the load vector and $\mathbf{u}$ is the nodal displacement vector. Double dot stands for the second derivative with respect to time, so that $\mathbf{\ddot{u}}$ means the nodal acceleration. Material damping is neglected. For the solution of equation (1), initial and boundary conditions (IC and BC) are needed. BC means prescribed displacement and traction in certain points or regions of the surface of the body. In dynamic problems when a body is moving freely, no BCs need to be defined. However, it is necessary to specify the ICs in order to calculate the first step of the temporal process. The initial conditions determine the position and velocity of the points of the body (or nodes of the FE model) in the very beginning of the examined time period.

$$\mathbf{u}(t) = \mathbf{u}_0 \qquad\qquad (t = 0) \tag{2}$$

and

$$\mathbf{\dot{u}}(t) = \mathbf{v}_0 \qquad\qquad (t = 0) \tag{3}$$

where $\mathbf{u}_0$ is the initial displacement and $\mathbf{v}_0$ is the initial velocity. At this point, it is important to note that as the effect of discretization, the model has finite number of eigenfrequencies, the same number as the degrees of freedom (DOF) of the model. In contrast to this, a continuous body has infinite number of eigenfrequencies. Consequently, the eigenfrequencies that are higher than the highest eigenfrequency of the discretized model are missing from the solution of the temporal process. Hence, independently from the applied time stepping method, spurious high frequency oscillations will occur in the results.

In the following subsections, five well known and widely used time stepping methods will be presented and analyzed. When a time stepping method is applied, the time period in consideration is subdivided into smaller time intervals. At the boundaries of the time intervals (in the "time steps"), the displacement, velocity and acceleration can be calculated from the displacement, velocity and acceleration at the previous time steps using the length of the time intervals (the "time step size"). In the investigated methods, the full time period will be subdivided into equally long Δt time intervals. For the sake of simplicity, at the end of ith time step the displacement $\mathbf{u}(i\Delta t)$ will be denoted by $\mathbf{u}_i$. Similar notation will be applied for the velocity and acceleration.

2.1. Newmark Method

The Newmark method is basically an implicit time stepping method which means that a state of the system at a later time step can be calculated from the state of the system in both the current and later time which results quite high computational costs. Displacements and velocities are given by the following equations [8].

$$\mathbf{u}_{i+1} = \mathbf{u}_i + \dot{\mathbf{u}}_i \Delta t + \left[\left(\frac{1}{2} - \beta\right)\ddot{\mathbf{u}}_i + \beta \ddot{\mathbf{u}}_{i+1}\right]\Delta t^2 \tag{4}$$

$$\dot{\mathbf{u}}_{i+1} = \dot{\mathbf{u}}_i + [(1-\gamma)\ddot{\mathbf{u}}_i + \gamma\ddot{\mathbf{u}}_{i+1}]\Delta t \tag{5}$$

With the proper choice of the two parameters β and γ, the order of accuracy and the dissipation can be controlled. The method is second order accurate if $\gamma \leq 1/2$ relation is fulfilled. However, if higher frequencies are damped out, the choice of parameter γ must be greater than $1/2$. The method is numerically stable if

$$\beta \geq \frac{1}{4}(1 + \delta)^2 \qquad \text{and} \qquad \gamma = \frac{1}{2} + \delta \tag{6}$$

where $\delta \geq 0$ is a new, but not independent parameter. If δ is zero, then the Newmark method has no numerical dissipation. With increasing δ values, the dissipation also increases. Let us write the equation of motion (1) in the later time step.

$$\mathbf{M}\ddot{\mathbf{u}}_{i+1} + \mathbf{K}\mathbf{u}_{i+1} = \mathbf{f}_{i+1} \tag{7}$$

Equations (4), (5) and (7) determines a system of equations from which the motion can be calculated from time step to time step. In order to analyze this method, the displacement, velocity and acceleration at the later time step should be rearranged to the left side of the equations. This system of equations can be written in matrix form as follows.

$$\begin{bmatrix} \mathbf{I} & \mathbf{0} & -\Delta t^2\beta\mathbf{I} \\ \mathbf{0} & \mathbf{I} & -\Delta t\gamma\mathbf{I} \\ \mathbf{K} & \mathbf{0} & \mathbf{M} \end{bmatrix}\begin{bmatrix} \mathbf{u}_{i+1} \\ \dot{\mathbf{u}}_{i+1} \\ \ddot{\mathbf{u}}_{i+1} \end{bmatrix} = \begin{bmatrix} \mathbf{I} & \Delta t\mathbf{I} & \Delta t^2(\frac{1}{2}-\beta)\mathbf{I} \\ \mathbf{0} & \mathbf{I} & \Delta t(1-\gamma)\mathbf{I} \\ \mathbf{0} & \mathbf{0} & \mathbf{0} \end{bmatrix}\begin{bmatrix} \mathbf{u}_i \\ \dot{\mathbf{u}}_i \\ \ddot{\mathbf{u}}_i \end{bmatrix} + \begin{bmatrix} \mathbf{0} \\ \mathbf{0} \\ \mathbf{f}_{i+1} \end{bmatrix} \tag{8}$$

where $\mathbf{I}$ means the unit matrix with the same size as $\mathbf{M}$ or $\mathbf{K}$. Assuming free vibrations, i.e., when $\mathbf{f} = \mathbf{0}$ in Eq. (1), the mode shape vectors of the system can be determined. The displacements, velocities and accelerations of the system can be given by the linear combination of mode shape vectors. The linear combination of them can be written in matrix form.

$$\mathbf{u} = \mathbf{Q}\mathbf{q} \tag{9}$$

where the columns of $\mathbf{Q}$ contain the mode shape vectors normalized to the mass matrix and the elements of $\mathbf{q}$ are the amplitudes of modal displacements. After substituting (9) into the equation of motion (1) and multiplying it by $\mathbf{Q}^T$ from the left, the system of equation splits into independent equations:

$$\begin{aligned}
\ddot{q}_1 + \omega_1^2 q_1 &= f_1 \\
\ddot{q}_2 + \omega_2^2 q_2 &= f_2 \\
&\vdots \\
\ddot{q}_k + \omega_k^2 q_k &= f_k \\
&\vdots
\end{aligned} \tag{10}$$

where q_k is the amplitude of the k-th modal displacement and ω_k is the k-th eigenfrequency of the system. Substituting (9) into equations (4) and (5) and factor out the $\mathbf{Q}$ matrix also provides independent equations for q_k and its time derivatives. These and (10) together give a set of single degrees of freedom (SDOF) equation for every mode shape. Each of them can be written in a similar form as (8). Introducing the notations:

$$\mathbf{A}_1 = \begin{bmatrix} 1 & 0 & -\Delta t^2 \beta \\ 0 & 1 & -\Delta t \gamma \\ \omega^2 & 0 & 1 \end{bmatrix} \qquad \mathbf{A}_2 = \begin{bmatrix} 1 & \Delta t & \Delta t^2 (\frac{1}{2} - \beta) \\ 0 & 1 & \Delta t(1 - \gamma)1 \\ 0 & 0 & 0 \end{bmatrix} \tag{11}$$

$$\mathbf{x} = \begin{bmatrix} q \\ \dot{q} \\ \ddot{q} \end{bmatrix} \qquad \mathbf{b} = \begin{bmatrix} 0 \\ 0 \\ f \end{bmatrix} \tag{12}$$

the matrix equation (8) can be written in a simpler SDOF form

$$\mathbf{x}_{i+1} = \mathbf{A}\mathbf{x}_i + \mathbf{b}_{i+1} \tag{13}$$

where $\mathbf{A} = \mathbf{A}_1^{-1}\mathbf{A}_2$. (Subscript indices were omitted.) Here the matrix $\mathbf{A}$ is the *amplification matrix* of the system which is a fundamental quantity for the definition of indicators characterizing the numerical method. In the following three sections, similar amplification matrices are going to be determined for further numerical methods.

2.2. Hilber–Hughes–Taylor Method

The Hilber–Hughes–Taylor (HHT-α) method [9] is another scheme which is widely employed for solving the equation of motion of mechanical systems. High frequency oscillations can be damped out in the Newmark method, but lower modes are also affected. This method is actually the improved version of the Newmark method with controllable numerical dissipation. Introducing the α parameter in equation (7), the damping effect to lower frequencies can be reduced.

$$\mathbf{M}\ddot{\mathbf{u}}_{i+1} + (1 + \alpha)\mathbf{K}\mathbf{u}_{i+1} - \alpha\mathbf{K}\mathbf{u}_i = \mathbf{f}_{i+1} \tag{14}$$

The main benefit in relation to the Newmark scheme is that by this method a certain amount of numerical damping can be introduced without degrading the order of accuracy. Equation (14) together with (4) and (5) forms the HHT-α method. Beside unchanged β and γ values, the amount of numerical damping can be controlled through the new parameter within the interval of $\alpha \in [-0.5\,,\,0]$ in which the smaller value of α means the smaller amount of dissipation. Rearranging equations

(4), (5) and (14) in matrix form and applying the modal transformation (9) separates the multi degrees of freedom (MDOF) equations into SDOF equations similar to (13). The amplification matrix is composed as $\mathbf{A} = \mathbf{A}_1^{-1}\mathbf{A}_2$ where $\mathbf{A}_1$ and $\mathbf{A}_2$ will be extended by α as follows:

$$\mathbf{A}_1 = \begin{bmatrix} 1 & 0 & -\Delta t^2\beta \\ 0 & 1 & -\Delta t\gamma \\ (1+\alpha)\omega^2 & 0 & 1 \end{bmatrix} \qquad \mathbf{A}_2 = \begin{bmatrix} 1 & \Delta t & \Delta t^2\left(\frac{1}{2}-\beta\right) \\ 0 & 1 & \Delta t(1-\gamma)1 \\ \alpha\omega^2 & 0 & 0 \end{bmatrix} \quad (15)$$

2.3. Backward Euler Method

The backward Euler (BE) scheme is the backward increment method with the simplest formulation. Due to its implicit character, similarly to the previous methods, a system of equations needs to be solved for every time step. This method is unconditionally stable, first order accurate and has a certain amount of numerical damping. The main problem is that the dissipation level is not controllable, hence it often leads to energy dissipation of an undesirable rate. Here, the displacement and velocity can be calculated as follows:

$$\mathbf{u}_{i+1} = \mathbf{u}_i + \dot{\mathbf{u}}_{i+1}\Delta t \tag{16}$$

$$\dot{\mathbf{u}}_{i+1} = \dot{\mathbf{u}}_i + \ddot{\mathbf{u}}_{i+1}\Delta t \tag{17}$$

Equations (16), (17) and (7) gives the system of equations to be solved. After performing the same transformations as in the previous sections, i.e., writing equations (16), (17) and (7) in matrix form and substituting equation (9) into them, a SDOF system of equations will be the result:

$$\mathbf{x}_{i+1} = \mathbf{A}\mathbf{x}_i + \mathbf{b}_{i+1} \tag{18}$$

where $\mathbf{x}$ and $\mathbf{b}$ are the same as in (12), while $\mathbf{A} = \mathbf{A}_1^{-1}\mathbf{A}_2$

$$\mathbf{A}_1 = \begin{bmatrix} 1 & -\Delta t & 0 \\ 0 & 1 & -\Delta t \\ \omega^2 & 0 & 1 \end{bmatrix} \qquad \mathbf{A}_2 = \begin{bmatrix} 1 & 0 & 0 \\ 0 & 1 & 0 \\ 0 & 0 & 0 \end{bmatrix} \tag{19}$$

2.4. Central Difference Method

The CDM, in contrast to the previously presented schemes, is an explicit time stepping method. The main benefits of using CDM are that it is second order accurate, quite simple to apply and, moreover, computations can be executed very fast due to its simple, explicit formulation. However, the central difference method is only conditionally stable which reduces the applicable time step region. In this method, the velocity and the acceleration are given using the displacement at the current, previous and next time step the following way:

$$\dot{\mathbf{u}}_i = \frac{\mathbf{u}_{i+1}-\mathbf{u}_{i-1}}{2\Delta t} \tag{20}$$

$$\ddot{\mathbf{u}}_i = \frac{\mathbf{u}_{i+1} - 2\mathbf{u}_i + \mathbf{u}_{i-1}}{\Delta t^2} \tag{21}$$

Another important property of the CDM is that it has no numerical damping effect. For the sake of comparability, a viscous damping term will be placed into the equation of motion which is applied in the current time step:

$$\mathbf{M}\ddot{\mathbf{u}}_i + \mathbf{C}\dot{\mathbf{u}}_i + \mathbf{K}\mathbf{u}_i = \mathbf{f}_i \tag{22}$$

where $\mathbf{C}$ is the damping matrix. After substituting (20) and (21) into (22) a linear system of equation will be deduced for $\mathbf{u}_{i+1}$:

$$(2\mathbf{M} + \Delta t\mathbf{C})\mathbf{u}_{i+1} = (4\mathbf{M} - 2\Delta t^2\mathbf{K})\mathbf{u}_i + (\Delta t\mathbf{C} - 2\mathbf{M})\mathbf{u}_{i-1} + 2\Delta t^2\mathbf{f}_i \tag{23}$$

If the coefficient matrix in (23) were diagonal, then the solution of the system of equation would be very simple and fast. The mass matrix can be diagonalizable by using lumped masses, but the damping matrix $\mathbf{C}$ stays unchanged. However, with a minor change of equation (20), the matrix $\mathbf{C}$ can be removed from the left side of equation. Let us write equation (20) only for the current and previous time steps.

$$\dot{\mathbf{u}}_i = \frac{\mathbf{u}_i - \mathbf{u}_{i-1}}{\Delta t} \tag{24}$$

Now, substitution of equations (24) and (21) into (22) provides a system of equation where the coefficient matrix can easily be transformed into a diagonal matrix.

$$\mathbf{M}\mathbf{u}_{i+1} = (2\mathbf{M} - \Delta t\mathbf{C} - \Delta t^2\mathbf{K})\mathbf{u}_i + (\Delta t\mathbf{C} - \mathbf{M})\mathbf{u}_{i-1} + \Delta t^2\mathbf{f}_i \tag{25}$$

Diagonal matrices can be inverted with very low computational costs. In case of zero damping matrix, CDM has no damping effect. The bulk viscosity is based on the CDM and uses a damping matrix proportional to the stiffness matrix.

$$\mathbf{C} = c_d\mathbf{K}$$

where c_d is the proportionality factor. Let us transform equation (25) into a more compact matrix form:

$$\begin{bmatrix} \mathbf{M} & \mathbf{0} \\ \mathbf{0} & \mathbf{I} \end{bmatrix} \begin{bmatrix} \mathbf{u}_{i+1} \\ \mathbf{u}_i \end{bmatrix} = \begin{bmatrix} 2\mathbf{M} - \Delta t\mathbf{C} - \Delta t^2\mathbf{K} & \Delta t\mathbf{C} - \mathbf{M} \\ \mathbf{I} & \mathbf{0} \end{bmatrix} \begin{bmatrix} \mathbf{u}_i \\ \mathbf{u}_{i-1} \end{bmatrix} + \begin{bmatrix} \Delta t^2\mathbf{f}_i \\ \mathbf{0} \end{bmatrix} \tag{26}$$

After substituting the transformation of (9) into (26), a SDOF will be obtained. For this, let us apply the results from the transformation of the system of equations (22).

$$\begin{aligned}
\ddot{q}_1 + 2\xi_1\omega_1\dot{q}_1 + \omega_1^2 q_1 &= f_1 \\
\ddot{q}_2 + 2\xi_2\omega_2\dot{q}_2 + \omega_2^2 q_2 &= f_2 \\
&\vdots \\
\ddot{q}_k + 2\xi_k\omega_k\dot{q}_k + \omega_k^2 q_k &= f_k \\
&\vdots
\end{aligned} \tag{27}$$

where ξ_k is the physical damping ratio belongs to the kth eigenfrequency ω_k. Similarly, as it has been conducted in the previous sections, new quantities can be introduced as follows:

$$\mathbf{A}_1 = \begin{bmatrix} 1 & 0 \\ 0 & 1 \end{bmatrix} \qquad \mathbf{A}_2 = \begin{bmatrix} 2 - 2\Delta t\omega\xi - \Delta t^2\omega^2 & 2\Delta t\omega\xi - 1 \\ 1 & 0 \end{bmatrix} \qquad (28)$$

and

$$\mathbf{x}_i = \begin{bmatrix} q_i \\ q_{i-1} \end{bmatrix} \qquad \mathbf{b}_i = \begin{bmatrix} \Delta t^2 f_i \\ 0 \end{bmatrix} \qquad (29)$$

The amplitudes of the modal displacement concerning to the next time step can be expressed in a simple matrix equation:

$$\mathbf{x}_{i+1} = \mathbf{A}\mathbf{x}_i + \mathbf{b}_i \qquad (30)$$

where $\mathbf{A} = \mathbf{A}_1^{-1}\mathbf{A}_2$

3 Accuracy Analysis

In order to analyze the stability and the numerical damping of the applied methods, two indicators are used which are the *spectral radius* and the *algorithmic damping ratio*. A method is said to be stable if the amplitude of modal displacements, i.e., $\mathbf{x}_{i+1}$ in (13), (18) or (30) stays finite even if i goes to infinity. It means that $\mathbf{x}_{i+1}$ have to be substituted back into $\mathbf{x}_i$ in (13), (18) and (30) in each time step which results the ith power of A. If $\mathbf{x}_0$ is the initial value, then:

$$\mathbf{x}_i = \mathbf{A}^i\mathbf{x}_0 + \sum_{k=1}^{i-1} \mathbf{A}^{i-k}\mathbf{b}_{k-p} + \mathbf{b}_{i-p} \qquad (31)$$

where $p = 0$ in the case of Newmark, HHT-α and BE methods and $p = 1$ in the case of CDM. The amplitudes of modal displacements stay finite if the absolute value of the greatest eigenvalue of the amplification matrix $\mathbf{A}$ is less than or equals one:

$$\rho(\mathbf{A}) = \max(|\lambda_j|) \le 1 \qquad (32)$$

where ρ is the spectral radius and λ_j is the j-th eigenvalue of $\mathbf{A}$. The algorithmic damping ratio is similar to the viscous damping, but without the viscous damping coefficient (c_d). Damped vibrations can be described by one of the differential equations (27). As first step, let us consider the exact solution of a damped vibration without the excitation force:

$$q(t) = c_1 e^{(-\xi+i\sqrt{1-\xi^2})\omega t} + c_2 e^{(-\xi-i\sqrt{1-\xi^2})\omega t} \qquad (33)$$

where c_1 and c_2 can be determined based on the initial conditions. For the sake of comparison with the discrete solution, let us divide the time interval equally into small Δt time steps. At the n-th step, the time is $t_n = n\Delta t$ and the solution is

$$q(t_n) = c_1\alpha_1^n + c_2\alpha_2^n \qquad (34)$$

Where $\alpha_1 = e^{(-\xi+i\sqrt{1-\xi^2})\Omega}$, $\alpha_2 = e^{(-\xi-i\sqrt{1-\xi^2})\Omega}$ and $\Omega = \omega\Delta t$. If $|\alpha_1| \leq 1$ and $|\alpha_2| \leq 1$ then the solution is stable. In the discrete solution, these quantities will be known as complex numbers in algebraic form:

$$\alpha_{1,2} = a \pm ib \tag{35}$$

The physical damping ratio ξ can be determined as:

$$\xi = -\frac{\ln(a^2+b^2)}{2\Omega} \tag{36}$$

Where,

$$\Omega\sqrt{1-\xi^2} = \arctan\left(\frac{b}{a}\right) \tag{37}$$

Equation (36) and (37) form a system of equations from which ξ can be solved.

Those numerical methods where no physical damping is present, but dissipation of energy can be observed, can be characterized by the algorithmic damping ratio. To determine this quantity, the amplification matrix of the method is needed. In the previous section this was derived for some well-known algorithms. Similar to (31) but without excitation:

$$\mathbf{x}_n = \mathbf{A}^n\mathbf{x}_0 \tag{38}$$

gives the time evolution of the algorithm with a given time step Δt. Transforming (38) to the coordinate system of the eigenvectors of $\mathbf{A}$ will lead to such an equation as (34), but $\alpha_{1,2}$ will be replaced with the eigenvalues of the amplification matrix $\lambda_{1,2}$. Here, the role of $\lambda_{1,2}$ is the same that of $\alpha_{1,2}$ was in (34). Hence, with $\lambda_{1,2} = a \pm ib$ the algorithmic damping ratio $\bar{\xi}$ can be solved with the following system of equations:

$$\bar{\xi} = -\frac{\ln(a^2+b^2)}{2\bar{\Omega}} \tag{39}$$

$$\bar{\Omega}\sqrt{1-\bar{\xi}^2} = \arctan\left(\frac{b}{a}\right) \tag{40}$$

Here, the unknowns $\bar{\xi}$ and $\bar{\Omega}$ are the algorithmic counterparts of ξ and Ω, respectively. Thus, knowing the amplification matrix, both the spectral radius and the algorithmic damping ratio can be determined.

4   Numerical Example

4.1.   Finite Element Model

Consider a one-dimensional problem where an elastic body (rod) collides with a rigid obstacle. This is a very simple problem, but the phenomena observed here are

also present in higher dimension cases. It is assumed that the displacements and strains are small and the rod exhibits linear elastic behavior. The centroidal axis of the rod coincides the x axis of the coordinate system (see Fig. 1).
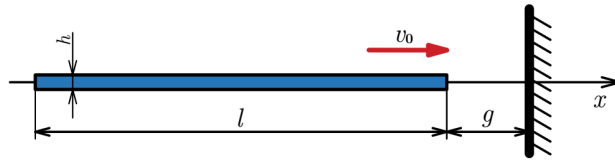
The rod moving towards the obstacle with constant v_0 velocity

In order to solve this test example, a FE model must be constructed based on the mechanical model shown in Fig. 1. This FE model is compiled from 1D truss elements (Fig. 2) which have 2 nodes with 1 DOF per node which is the longitudinal displacement. The FE model constructed from these element types is shown in Fig. 3.
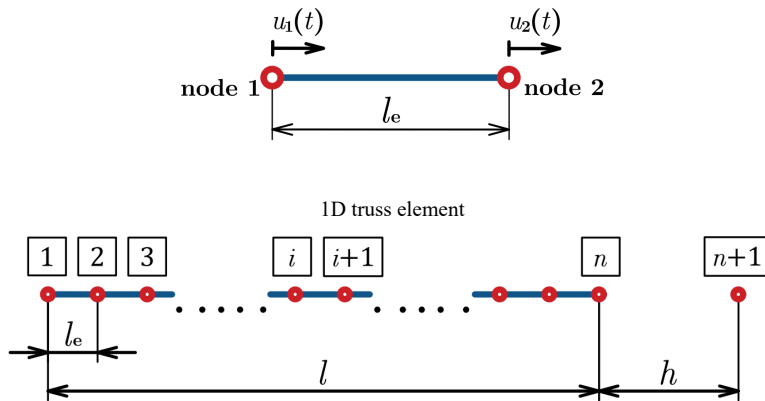
1D truss element

FE model

According to Fig. 3 the stiffness matrix of the structure is assembled from the element level stiffness matrices.

$$
K = \begin{bmatrix}
k & -k & \dots & & & & 0 \\
-k & 2k & -k & & & & \\
\vdots & -k & \ddots & & & & \vdots \\
& & & 2k & -k & & \\
& & & -k & k & 0 & \\
0 & & \dots & & 0 & 1
\end{bmatrix}
\tag{41}
$$

where the stiffness matrix of one two-noded truss element is

$$
K^e = \begin{bmatrix} k & -k \\ -k & k \end{bmatrix}
\tag{42}
$$

and

$$k = \frac{AE}{l_e} \tag{43}$$

where A is the area of the cross section, E is the modulus of elasticity and l_e is the length of the truss element. Because of the initial gap h, the rod will reach the wall after $t_0 = v_0/h$ time.

4.2. Treatment of the Contact

The proper handling of the contact is an important aspect to be considered in the modeling. As it has been mentioned in Section 1, there are two widely used approaches which are the penalty method and the Lagrange multiplier method. In this paper, the latter approach is used. Thus, the penetration between the contacted bodies is completely prohibited. The prevalent displacement constraints are prescribed the following way.

$$\mathbf{G}(\mathbf{u} + \mathbf{X}) = \mathbf{0} \tag{44}$$

where $\mathbf{X}$ means the initial configuration (vector of length $n + 1$ filled with the initial coordinates of nodes) and $\mathbf{G}$ is the contact constraint matrix. Equation (44) describes the Hertz-Signorini-Moreau (HSM) conditions [3]. The detailed description of this formulation can be found in [26]. The equation of motion (1) must be modified with regard to the contact force acting between the elastic rod and the rigid wall. Thus, it can be written as

$$\mathbf{M}\ddot{\mathbf{u}} + \mathbf{K}\mathbf{u} + \mathbf{G}^{\mathrm{T}}\lambda = \mathbf{f} \tag{45}$$

where λ denotes the Lagrange multiplier which is equivalent with the surface contact pressure. Thus, (44) and (45) must be considered as a system of equations treating λ as unknown. The numerical methods examined in section 2 can easily be deducted for the contacting case by replacing the equation of motion (1) with (45). As the additional term in (45) does not depend on the displacement or its derivatives, the $\mathbf{A}_1$ and $\mathbf{A}_2$ matrices presented in section 2 remain unchanged.

5 The Proposed Method

The common way of reducing the spurious oscillations in a contact problem is to apply a numerical method which has numerical damping. From the examined methods that have been described in Section 2, the BE, Newmark and HHT methods both possess this property. By the latter two, the numerical damping can be altered using one or two parameters, respectively. This is a very important attribute, as disadvantageous, damping characteristics can distort the resulting functions (contact pressure, velocity, etc.).

The proposed method uses a significantly different approach compared to the above-mentioned methods. Here, the damping effect is exerted via viscous damping. From this aspect, it is similar to the bulk viscosity method, so the proposed method can be considered an improved version of it. The basic numerical method which is coupled with a specific damping is the CDM. Hence, matrix $\mathbf{C}$ in equation (22) will be nonzero in this case. The appropriate characteristics of the applied viscous damping in the function of the eigenfrequencies is very important. In contact problems, spurious oscillations mainly have high frequency components (above 10^6 Hz). Hence, it is beneficial to apply damping characteristics which provides a higher amount of damping in the high frequency regions. In order to achieve this, a progressive damping characteristic was chosen. The maximum of the damping character is ξ_{max} for the highest frequency ω_{max} and the initial slope of the curve is ξ_{min}/ω_{max} when ω is zero. It means that a vertical line starting from ω_{max} and crosses this slope at ξ_{min}. (See Fig. 4) A suitable function that satisfies these criteria is the following.

$$\bar{\bar{\xi}}(\omega) = c_1 \sinh(c_2 \omega) \tag{46}$$

where c_1 and c_2 are alterable parameters by which the concrete form of the damping curve can be adjusted. The values of these parameters can be determined from the previously mentioned conditions as:

$$\xi_{max} = c_1 \sinh(c_2 \omega_{max}) \tag{47}$$

and

$$\xi_{min} = c_1 c_2 \omega_{max} \tag{48}$$

If ξ_{min} and ξ_{max} are given, the appropriate values for c_1 and c_2 can be determined from (47) and (48). Applying (46) on ω_k each modal damping ratio ξ_k can be determined. After that, the system of equations (27) has to be transformed back to the physical space. Practically, it means that a diagonal matrix containing the terms $2\xi_k \omega_k$ in the kth row and column has to be multiplied by inverse of $\mathbf{Q}^T$ from left and inverse of $\mathbf{Q}$ from right to generate the damping matrix $\mathbf{C}$.

The damping characteristics for the methods introduced in Section 2 are presented in Fig. 4. The proposed damping curve is highly progressive compared to every other examined method. Table 1 provides a summary of the previously introduced methods.

For the sake of comparability, it is beneficial to set the methods with alterable damping (Newmark, HHT-α, bulk viscosity) to the same energy dissipation level as the proposed method has. Let $E^{TOTAL}(t_0)$ denote the total energy of the rod at the beginning and $E^{TOTAL}(t_{max})$ the total energy at the end of the investigated time interval.
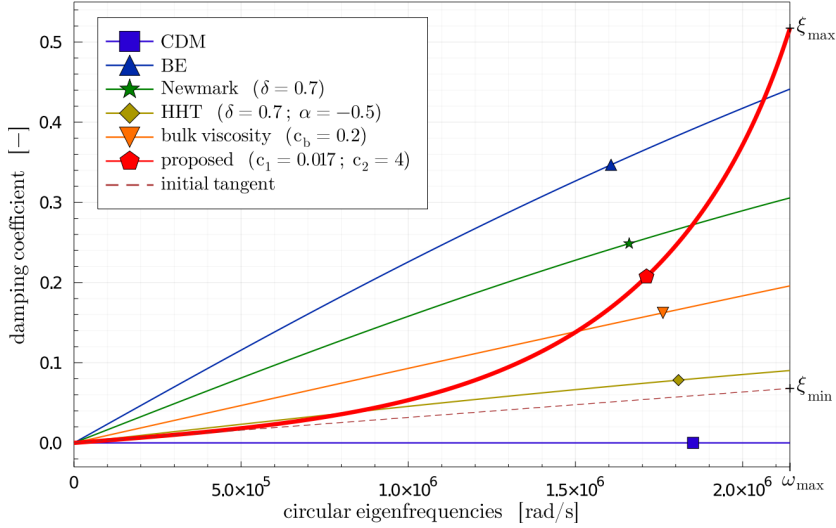
Damping ratio for the examined methods

The parameters in Newmark, HHT-α, bulk viscosity and the proposed method have been chosen so that:

$$\Delta E^{TOTAL} = E^{TOTAL}(t_{max}) - E^{TOTAL}(t_0) \tag{49}$$

is the same for each method. This setting is applied in Fig. 5 where the spectral radius is presented which is another important accuracy measure (see Section 3). The time step size Δt has been chosen to be 50% of the critical time step size. The spectral radii of the CDM and the proposed method were solved for the highest eigenfrequency. Smaller parameter values provide more accurate results for Newmark and HHT-α methods, but deteriorate the efficiency. It can be seen that by equal energy dissipation, the proposed method can exert much more damping at the highest eigenfrequency by the applied time step. However, the proposed method is only conditionally stable, i.e., beyond the critical time step the spectral radius oversteps one. Nevertheless, in contact problems, this is not problematic, as a very dense discretization is needed in time to provide an acceptable resolution in the resulting functions.

Table 1

Summary of the applied numerical methods

method	parameters	implicit/explicit	damping character
CDM	-	explicit	zero
BE	-	implicit	degressive
Newmark	β, γ	implicit	degressive
HHT-α	α, β, γ	implicit	degressive

bulk viscosity	c_b	explicit	linear
proposed	c_1, c_2	explicit	progressive
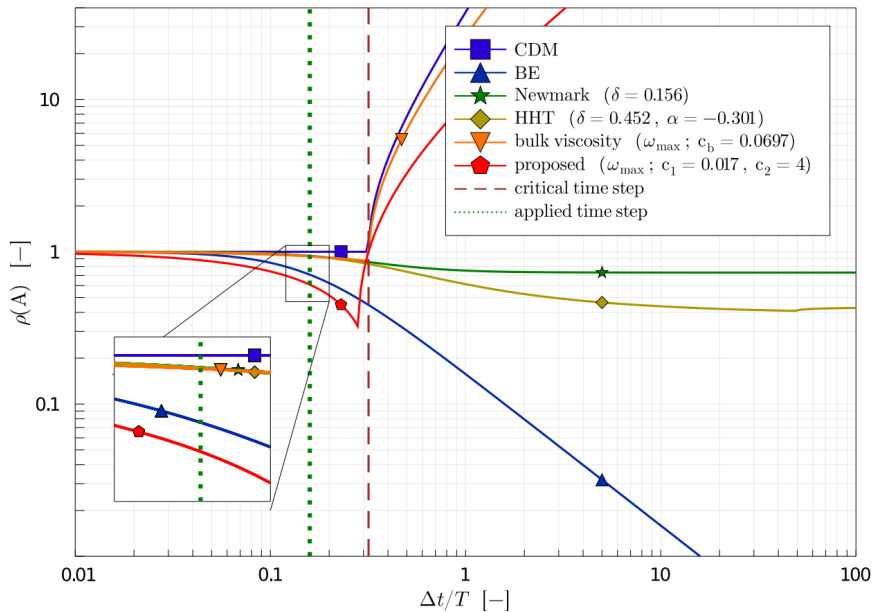
Figure 5
Spectral radii of the examined methods

6 Application to the One-Dimensional Example

The efficiency of the proposed method can be proved by the solution of the 1D example described in Section 4. The spurious oscillations are mainly problematic in the time evolution of the velocity and the pressure. The former quantity is shown in Fig. 6 where the same parameter setting is applied as in Fig. 5. It can be seen that right after the impact, the proposed method does not result any oscillations. Moreover, it runs the closest to the exact solution which means that it is more accurate, than any of the other methods. The bump in the top right zoomed subplot is present due to the wave propagation in the rod. Here, the slightest possible bump is desirable for the accurate solution. It can be seen that the proposed method is the most accurate from this aspect as well.

Examination of the time evolution of contact pressure presented in Fig. 7 is also very important. Using the proposed method, the oscillations can be terminated very effectively. Right after the impact, the proposed method provides far the best

solution. Right before the separation, the sheer central difference method runs closer to the exact solution. However, the proposed method surpasses all the other methods even in this region.
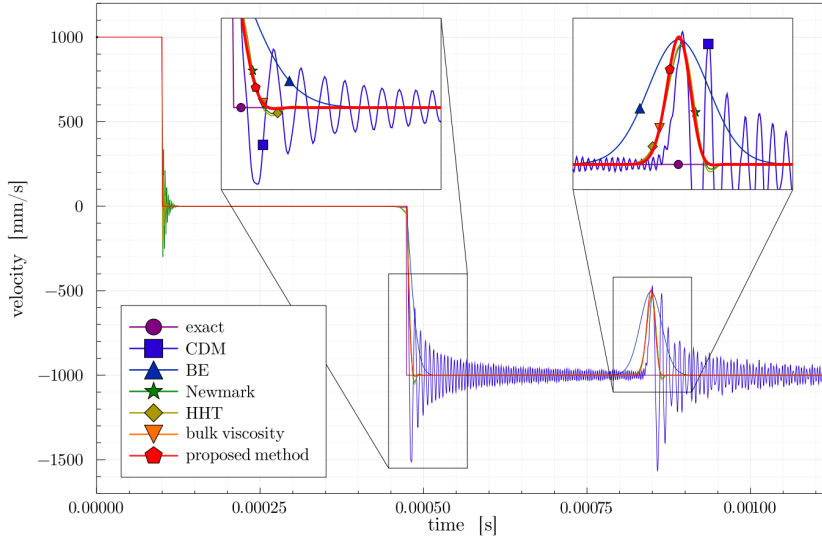
Figure 6
Time evolution of the velocity at the contacting node
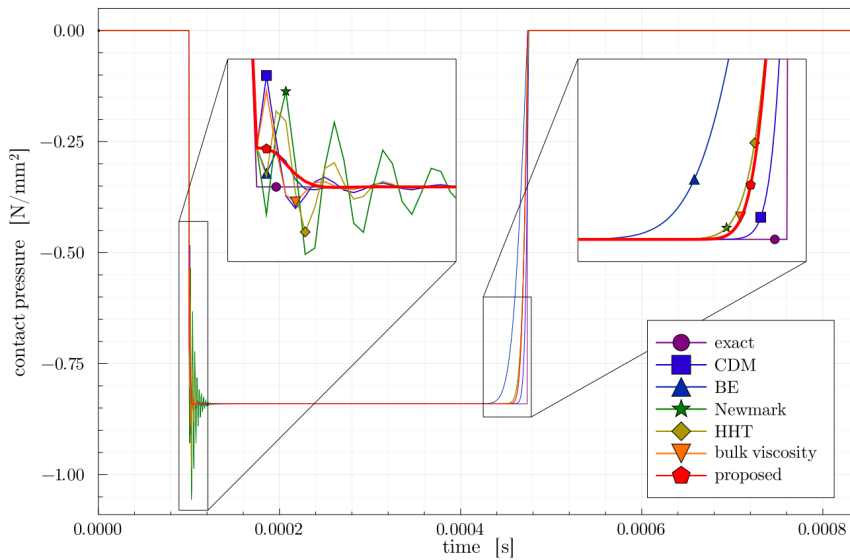
Figure 7
Time evolution of the contact pressure

For the illustration of the efficiency of results, five indicators have been defined. The first one is the relative error of the contact pressure. Since the exact solution of the problem is known, the relative error can be determined as:

$$\varepsilon_p = \frac{\sum_{i=1}^{n_t} |p_i^{EXACT} - p_i^{FEM}|}{\sum_{i=1}^{n_t} |p_i^{EXACT}|} \tag{50}$$

where n_t is the number of the time steps and $p_i^{\blacksquare}$ means the contact pressure at the i-th time step both for the case of exact and FE solution. The second indicator is the total variation of the contact pressure:

$$V_p = \sum_{i=1}^{n_t - 1} |p_{i+1}^{FEM} - p_i^{FEM}| \tag{51}$$

These two indicators can be applied for the velocities of the nodes of finite elements as well, just the letter p have to be replaced by v in equation (50) and (51). The third indicator is the number of the peaks in the graph of the contact pressure or the nodal velocity. The fourth indicator is the rate of drop of the total energy of the rod during the process:

$$\delta_e = \frac{E_{n_t}^{TOTAL} - E_1^{TOTAL}}{E_1^{TOTAL}} \tag{52}$$

where $E_{\blacksquare}^{TOTAL}$ means the total energy of the rod in different time steps. If the parameters of the method allow it, this has been chosen so that the drop of the total energy would be the same (see Fig. 10). It makes the comparison easier among the methods. The last indicator was the duration of the calculation. Fig. 8 shows that the proposed method provides the best total variation and the least wave peak number for the contact pressure. The second order accurate CDM gives the smallest relative error, but the proposed method provides the second-best solution. The same indicators for the velocity of the contacting node at the right end of the rod can be seen in Fig. 9. The total variation and the relative error for the bulk viscosity method are slightly better, but the number of wave peak is by far the best for the proposed method.
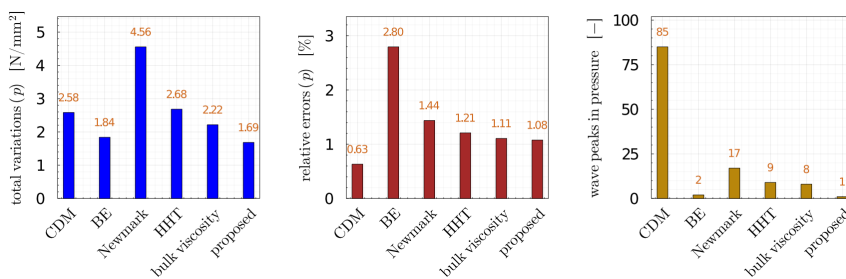
Figure 8

Total variation, relative error and the number of wave peaks for the contact pressure
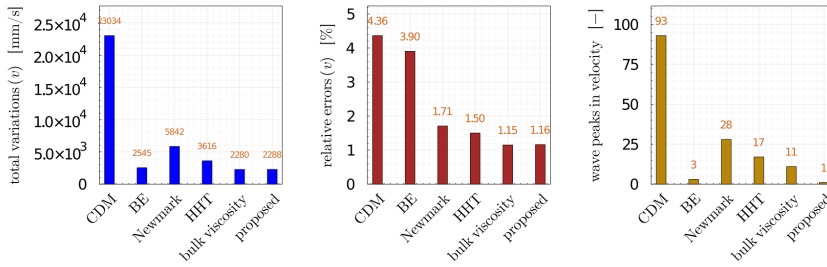
Figure 9

Total variation, relative error and the number of wave peaks for the velocity of the contacting node at the right end of the rod
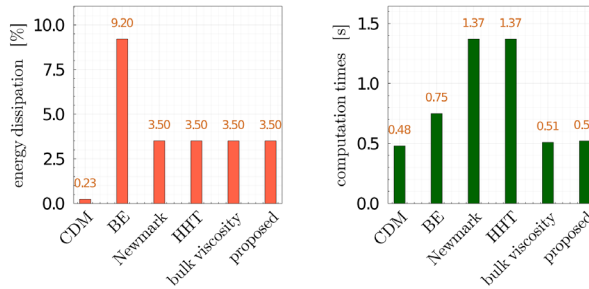
Figure 10

Energy dissipation and computation times for the applied methods

Finally, the computation time of methods with explicit formulation, i.e., the CDM and the proposed method are almost the same, but much less than the implicit ones (see Fig. 10). On this basis, it can be stated that the proposed method provides the least oscillating but the most accurate results among the dissipative time stepping methods.

Conclusions

In this article, a novel approach was presented for solving dynamic contact problems effectively. The proposed method is based on the central difference method and includes damping effect exerted, as viscous damping. Based on the conducted numerical tests, the concrete shape of the damping curve has an important role to reduce spurious oscillations effectively. The damping curve of the here presented approach is defined based on the specific formulation of the $\text{sh}(x)$ function. The included numerical results prove that spurious oscillations can be reduced more effectively, with the applied damping character, than by using existing numerical methods. Although, the examined 1D contact problem is very simplistic, the phenomena that appears, have similarities found in higher dimension cases. Thus, these successful tests suggest that the proposed method can be applicable for more complex problems. The extension of our method, to two-dimensional problems, is in progress, results are going to be published in the near future. In addition,

investigations on the efficacy of other types of damping characteristics is also being planned.

References

[1]   H. Hertz, On the contact of elastic solids, Z. Reine Angew. Mathematik 92 (1881) 156-171

[2]   A. Francavilla, O. Zienkiewicz, A note on numerical computation of elastic contact problems, International Journal for Numerical Methods in Engineering 9 (4) (1975) 913-924

[3]   P. Wriggers, Computational Contact Mechanics, John Wiley&Sons, 2002

[4]   K. Willner, L. Gaul, A penalty approach for contact description by fem based on interface physics, WIT Transactions on Engineering Sciences 7 (1970)

[5]   P. Papadopoulos, J. Solberg, A lagrange multiplier method for the finite element solution of frictionless contact problems, Mathematical and computer modelling 28 (4-8) (1998) 373-384

[6]   J. C. Simo, T. A. Laursen, An augmented lagrangian treatment of contact problems involving friction, Computers & Structures 42 (1) (1992) 97-116

[7]   T. Belytschko, T. J. Hughes, Computational methods for transient analysis, Amsterdam, North-Holland (Computational Methods in Mechanics 1 (1983)

[8]   N. M. Newmark, A method of computation for structural dynamics, Journal of the engineering mechanics division 85 (3) (1959) 67-94

[9]   H. M. Hilber, T. J. Hughes, R. L. Taylor, Improved numerical dissipation for time integration algorithms in structural dynamics, Earthquake Engineering & Structural Dynamics 5 (3) (1977) 283-292

[10]   S.-Y. Chang, Improved numerical dissipation for explicit methods in pseudo-dynamic tests, Earthquake Engineering & Structural Dynamics 26 (9) (1997) 917-929

[11]   G. Noh, S. Ham, K.-J. Bathe, Performance of an implicit time integration scheme in the analysis of wave propagations, Computers & Structures 123 (2013) 93-105

[12]   R. D. Krieg, S. W. Key, Transient shell response by numerical time integration, International Journal for Numerical Methods in Engineering 7 (3) (1973) 273286

[13]   D. J. Benson, Computational methods in lagrangian and eulerian hydrocodes, Computer methods in Applied mechanics and Engineering 99 (2-3) (1992) 235394

[14]   J. VonNeumann, R. D. Richtmyer, A method for the numerical calculation of hydrodynamic shocks, Journal of applied physics 21 (3) (1950) 232-237

[15] S. Hibbitt, Karlsson, Abaqus theory manual (v6.7), Inc of Pawtucket, Rhode Island (2007)

[16] J. O. Hallquist, Ls-dyna theoretical manual (v960), Livermore software technology corporation (1998)

[17] L. Maheo, G. Rio, V. Grolleau, On the use of some numerical damping methods of spurious oscillations in the case of elastic wave propagation, Mechanics Research Communications 38 (2) (2011) 81-88

[18] L. Maheo, V. Grolleau, G. Rio, Numerical damping of spurious oscillations: a comparison between the bulk viscosity method and the explicit dissipative tchamwa-wielgosz scheme, Computational Mechanics 51 (1) (2013) 109-128

[19] P.-S. B. Shing, S. A. Mahin, Elimination of spurious higher-mode response in pseudodynamic tests, Earthquake engineering & structural dynamics 15 (4) (1987) 425-445

[20] C. Kolay, J. M. Ricles, Development of a family of unconditionally stable explicit direct integration algorithms with controllable numerical energy dissipation, Erthquake Engineering & Structural Dynamics 43 (9) (2014) 1361-1380

[21] S.-Y. Chang, Discussion of paper 'development of a family of unconditionally stable explicit direct integration algorithms with controllable numerical energy dissipation'by chinmoy kolay and james m. ricles, earthquake engineering and structural dynamics 2014; 43: 1361-1380, Earthquake Engineering & Structural Dynamics 44 (2) (2015) 325-328

[22] W. Kim, A new family of two-stage explicit time integration methods with dissipation control capability for structural dynamics, Engineering Structures 195 (2019) 358-372

[23] H. Chen, Y. X. Zhang, M. Y. Zang, P. J. Hazell, An explicit lagrange constraint method for finite element analysis of frictionless 3d contact/impact problems, in: Applied Mechanics and Materials, Vol. 553, Trans Tech Publ, 2014, pp. 751-756

[24] B. Zhu, H. Li, An improved dynamic contact model for mass-spring and finite element systems based on parametric quadratic programming method, Latin American Journal of Solids and Structures 15 (2018)

[25] P. Otto, L. De Lorenzis, J. F. Unger, A regularized model for impact in explicit dynamics applied to the split hopkinson pressure bar, Computational Mechanics 58 (4) (2016) 681-695

[26] N. J. Carpenter, R. L. Taylor, M. G. Katona, Lagrange constraints for transient finite element surface